

1  
2 Inferring the differences in incubation-period and  
3 generation-interval distributions of the Delta and Omicron  
4 variants

## 5 **Abstract**

6 Estimating the differences in the incubation-period, serial-interval, and  
7 generation-interval distributions of SARS-CoV-2 variants is critical to  
8 understanding their transmission dynamics and outbreak control. However,  
9 estimating and comparing the timing of infection and transmission is inherently  
10 difficult due to the impact of epidemic dynamics—for example, when an epidemic is  
11 growing exponentially, a cohort of infected individuals who developed symptoms at  
12 the same time are more likely to have been infected recently. Here, we re-analyze  
13 incubation-period and serial-interval data describing transmissions of the Delta and  
14 Omicron variants from Netherlands at the end of December 2021. Previous analysis  
15 of the same data set reported shorter mean observed incubation period (3.2 days vs  
16 4.4 days) and serial interval (3.5 days vs 4.1 days) for the Omicron variant, but the  
17 number of infections caused by the Delta variant decreased during this period as  
18 the number of Omicron infections increased. When we account for the impact of  
19 growth-rate differences on inferences of two variants, we estimate similar mean  
20 incubation periods (3.8–4.5 days) for both variants but a shorter mean generation  
21 interval for the Omicron variant (3.0 days; 95% CI: 2.7–3.2 days) than for the Delta  
22 variant (3.8 days; 95% CI: 3.7–4.0 days). The differences in generation intervals  
23 may reflect higher effective reproduction numbers of the Omicron variant, which  
24 can drive faster susceptible depletion among close contacts. Using up-to-date  
25 generation-interval distributions is critical to accurately estimating the  
26 reproduction advantage of the Omicron variant.

# 1 Introduction

Estimating transmission advantages of new SARS-CoV-2 variants is critical to predicting and controlling the course of the COVID-19 pandemic. Transmission advantages of invading variants are typically characterized by the ratios of reproduction numbers,  $\mathcal{R}_{\text{inv}}/\mathcal{R}_{\text{res}}$ , and the differences in growth rates,  $r_{\text{inv}} - r_{\text{res}}$ . These two quantities are linked by the generation-interval distributions of the resident and invading variants. For example, an invading variant with shorter generation intervals—defined as the time between infection of the infector and the infectee—will exhibit faster epidemic growth ( $r_{\text{inv}} > r_{\text{res}} > 0$ ) even if their reproduction numbers are identical ( $\mathcal{R}_{\text{inv}} = \mathcal{R}_{\text{res}} > 1$ ).

Estimating the generation-interval distribution is challenging, in part, due to difficulties in observing actual infection events. Many researchers primarily focus on comparisons of other transmission intervals, such as the time between symptom onsets (also referred to as serial intervals) or between testing events [1] of the infector and the infectee. Each of these transmission-interval distributions are subject to dynamical effects which, can bias estimation. For example, when the epidemic is growing, a cohort of infectors who developed symptoms at the same time are more likely to have been infected recently—in other words, their incubation periods will be shorter, on average, than those of their infectees, causing the mean serial interval to be longer than the mean generation interval [2]. Therefore, observed differences in transmission-interval distributions between variants are not necessarily equivalent to differences in the underlying generation-interval distributions, especially if their growth rates differ.

Here, we re-analyze serial-interval data collected by [3], representing within- and between-household transmissions of the Delta and Omicron variants from the Netherlands between 13 and 26 December 2021. The study found shorter mean serial intervals (3.5 vs 4.1 days) and mean incubation periods (3.2 vs 4.4 days) for transmission pairs with S-gene target failure (mostly Omicron during the study period) than without (mostly Delta), but did not consider growth-rate differences in their inference: during this period, the Omicron cases were increasing, whereas the Delta cases were decreasing. Here, we take the epidemiological context in the Netherlands during the study period into account to provide corrected estimates for the incubation periods and generation-interval distributions of the Delta and Omicron variants. We show that using up-to-date generation-interval distributions is critical to accurately estimating the reproduction advantage (i.e., the ratio between the reproduction numbers of the invading and resident variants) of emerging SARS-CoV-2 variants.

## 2 Methods

### 2.1 Data

We analyze time series of reported COVID-19 cases (<https://data.rivm.nl/covid-19/>) and proportions of SARS-CoV-2 variants detected (<https://www.rivm.nl/coronavirus-covid-19/virus/varianten>) from the Netherlands between 29 November 2021 and 30 January 2022. Data sets are publicly available on the National Institute for Public Health and the Environment (RIVM) website.

Serial interval data are taken from [3] (see original article for details of data collection). The data are aggregated by the length of the serial interval in days and do not include additional individual-level information, such as exposure dates or symptom onset dates. The data consists of 2529 transmission pairs and are further stratified by the presence of S gene target failure (SGTF), week of infectors' symptom onset date (weeks 50 and 51 of 2021), and the type of transmission (within or between households). In the main text, we combine data from weeks 50 and 51 of 2021 and present a stratified analysis in Supplementary Material. For simplicity, we refer to transmission pairs with and without SGTFs as Omicron and Delta transmission pairs, respectively. Incubation period data are not publicly available with the original article; instead, we rely on previous estimates [3] to derive growth-rate-adjusted incubation-period distributions.

### 2.2 Estimating epidemic growth rates

In order to accurately estimate incubation-period and generation-interval distributions of the Delta and Omicron variants, we have to take their epidemiological dynamics—in particular, the differences in their growth rates—into account. To estimate the growth rates differences of the Delta and Omicron variants, we first estimate the number of COVID-19 cases caused by each variant by multiplying reported weekly numbers of cases by the proportion of Delta and Omicron variants detected—we use weekly time series to smooth over patterns of testing and reporting within each week. We then fit a generalized additive model [4] to the logged weekly case estimates to obtain smooth trajectories for case time series. Finally, we take the derivative of the predicted logged numbers of cases caused by each variant to obtain time-varying growth rate estimates.

To obtain confidence intervals on the estimated time-varying growth rates, we generate 1000 parameter sets by resampling spline coefficients from a multivariate normal distribution using the estimated variance-covariance matrices. We calculate time-varying growth rates from each parameter set and use equi-tailed quantiles to generate 95% confidence limits.

## 2.3 Estimating forward incubation-period distributions from backward incubation-period distributions

The incubation-period distributions from 513 individuals (258 Omicron and 255 Delta cases), with symptom onsets between 1 December 2021 and 2 January 2022, were previously reported in [3]. [3] used the methods of [5], which estimates incubation period by inferring distributions of time of infection for each individual from their known exposure dates, using a uniform distribution, and compares this to a known symptom-onset time.

In practice, incubation periods (and other epidemiological delays) can be measured in two ways: forward and backward [2]. The forward incubation periods are measured from a cohort of individuals who were infected at the same time. We expect this forward incubation-period distribution  $f_I(\tau)$  to remain constant over the course of an epidemic and provide reliable estimates of the distribution across individuals. Backward incubation periods are measured from a cohort of individuals who developed symptoms at the same time. The backward incubation-period distribution is sensitive to epidemic dynamics: the difference arises because forward incubation periods look forward from the reference point towards symptom development, which is an individual-level process, while backward incubation periods look backwards towards an infection event, which requires an interaction with an infectious individual.

In particular, when incidence of infection is growing exponentially, we are more likely to observe backward incubation periods that are shorter than the corresponding forward incubation periods because there will be relatively more individuals who were infected recently. Assuming that incidence is changing exponentially at a constant rate  $r$  across the study period, the backward incubation-period distribution  $b_I(\tau)$  corresponds to:

$$b_I(\tau) = \frac{\exp(-r\tau)f_I(\tau)}{\int_0^\infty \exp(-rx)f_I(x) dx}. \quad (1)$$

The method of [5] starts from observed symptom onsets, and estimates the backward incubation-period distribution without taking growth rates into account.

For a given growth rate  $r$ , the corresponding forward incubation-period distributions can be calculated by inverting Eq. (1):

$$f_I(\tau) = \frac{\exp(r\tau)b_I(\tau)}{\int_0^\infty \exp(rx)b_I(x) dx}. \quad (2)$$

Since incubation-period data are not provided, we are not able to fit Eq. (2) directly; instead we take the backward incubation-period distributions  $b_I(x)$  estimated by [3], which was originally assumed to follow a Weibull distribution, and apply Eq. (2). In particular, [3] estimated the scale and shape parameters of the Weibull distribution to be 4.93 (95% CI: 4.51–5.37) and 1.83 (95% CI: 1.59–2.08), respectively, for the non-SGTF cases, and 3.60 (95% CI: 3.23–3.98) and 1.50 ((95% CI: 1.32–1.70), respectively, for SGTF cases.

135 We also model the backward incubation-period distribution  $b_I(\tau)$  using a Weibull  
136 distribution based on the assumptions of [3]. To account for uncertainties in the orig-  
137 inal parameter estimates, we rely on a sampling scheme, similar to the one we used  
138 for the growth rate analysis (in Section 2.2). First, we approximate the previously  
139 inferred posterior distributions of the shape and scale parameters of the Weibull  
140 distribution using a lognormal distribution—we parameterize the lognormal distri-  
141 bution such that (i) its median matches the median of the posterior distributions and  
142 (ii) the probability that a random variable following the specified lognormal distri-  
143 bution falls between the lower and upper credible limits matches 95% [6]. We draw  
144 1000 samples of the shape and scale parameters (for the backward distribution  $b_I(\tau)$ )  
145 from the specified lognormal distributions and estimate the corresponding forward  
146 distribution using Eq. (2). We take 95% equi-tailed quantiles to obtain 95% confi-  
147 dence intervals. We repeat the analysis across plausible ranges of  $r$  for the Delta and  
148 Omicron variants separately (discussed later).

## 149 2.4 Estimating forward generation-interval distributions from 150 forward serial-interval distributions

151 Dynamical biases in the serial-interval distributions are more complex because the se-  
152 rial interval depends on the incubation periods of the infector and the infectee as well  
153 as the generation interval between them (Fig. 1). For example, [3] measured the for-  
154 ward serial-interval distributions from cohorts of infectors who developed symptoms  
155 during the same week. In this case, the forward serial interval  $\tau_s$  can be expressed  
156 in the form [2]:

$$\tau_s = -\tau_{i,1} + \tau_{g,\text{symp}} + \tau_{i,2}, \quad (3)$$

157 where  $\tau_{i,1}$  represents the backward incubation period of the infector (because all  
158 infectors developed symptoms at the same time), and  $\tau_{i,2}$ , represents the forward  
159 incubation period of the infectee. Here,  $\tau_{g,\text{symp}}$  represents the generation interval  
160 between the infector and the infectee; we use the subscript *symp* to indicate that  
161 these generation intervals are measured from infectors who developed symptoms at  
162 the same time.

The generation-interval distribution for a symptom-based cohort ( $\tau_{g,\text{symp}}$  in Eq. (3))  
is biased because infectors who developed symptoms at the same time will have  
shorter incubation periods (when the epidemic is growing) and therefore transmit  
earlier (Fig. 1A). This symptom-based generation-interval distribution depends on  
the backward incubation-period distribution:

$$f_{G,\text{symp}}(\tau) = \int_0^\infty f_{G|I}(\tau|x)b_I(x)dx, \quad (4)$$

where  $f_{G|I}(\tau|x)$  represents the forward generation-interval distribution conditional  
on a known value of the incubation period,  $x$ , and  $b_I(x)$  represents the backward  
incubation-period distribution. Instead, the forward generation-interval distribution

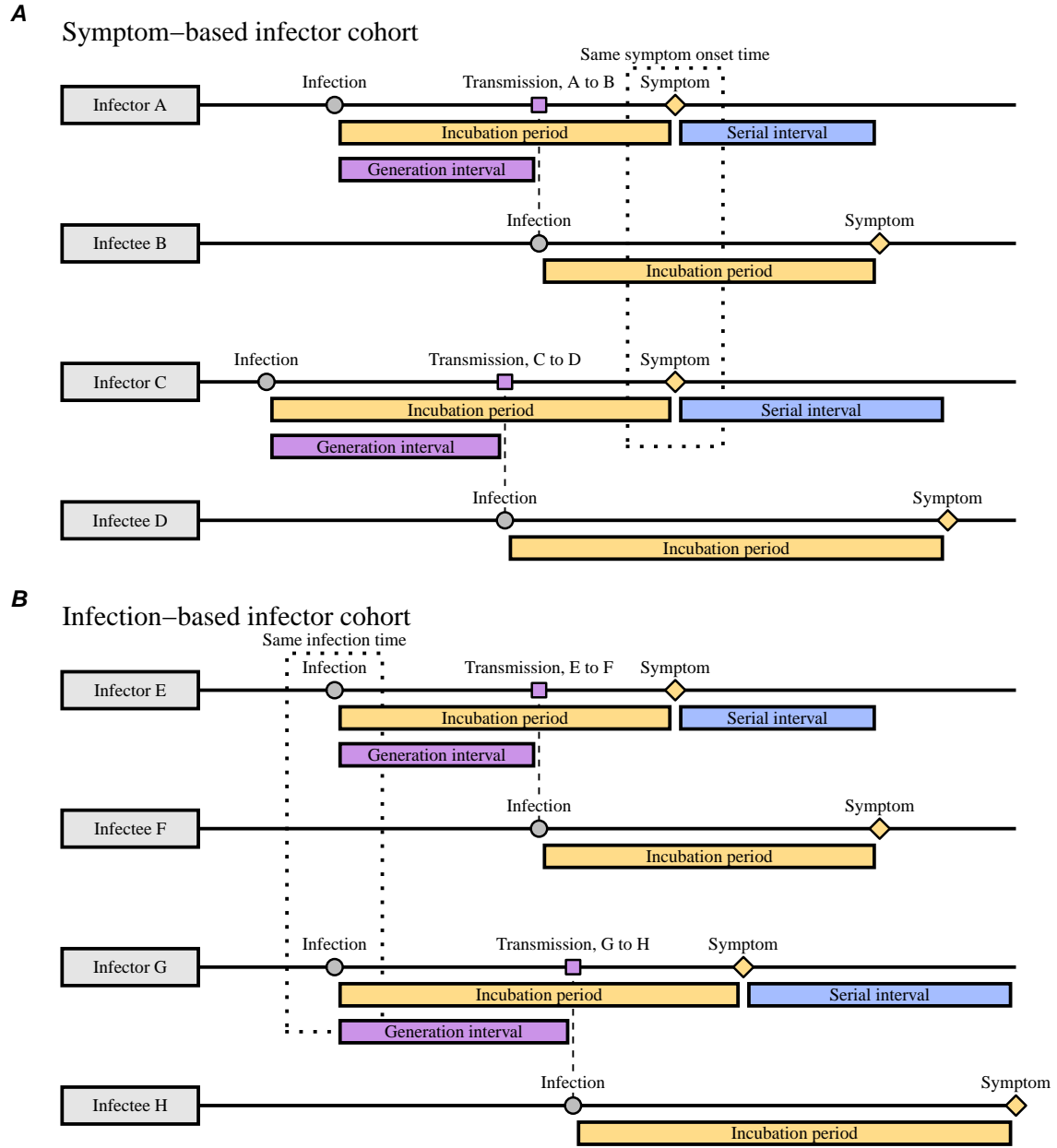


Figure 1: **Schematic diagrams of serial and generation intervals from symptom- and infection-based infector cohorts.** (A) Serial intervals are typically measured from the cohort of infectors who develop symptoms at the same time. In this case, infectors will have shorter incubation periods than their infectees on average; the corresponding generation intervals will be also short because infectors with short incubation periods will transmit earlier. (B) Generation intervals are better measured from the cohort of infectors who are infected at the same time because their incubation periods will be unbiased.

measured from a cohort of individuals who were infected at the time is expected to provide reliable estimates of the distribution across individuals (because their incubation-period distribution is expected to remain constant over time, Fig. 1B):

$$f_{G,\text{inf}}(\tau) = \int_0^\infty f_{G|I}(\tau|x)f_I(x) dx. \quad (5)$$

When an epidemic is growing exponentially, there are two opposing effects affecting the relationship between the mean serial and generation interval. First, infectors in a given cohort are more likely to have shorter incubation periods than their infectees on average,  $\mathbb{E}[\tau_{i,1}] < \mathbb{E}[\tau_{i,2}]$ , causing the mean forward serial interval to be longer than the mean symptom-based generation interval ( $\mathbb{E}[\tau_s] > \mathbb{E}[\tau_{g,\text{symp}}]$ ). Second, the mean symptom-based generation interval will be shorter than the mean infection-based generation interval:  $\mathbb{E}[\tau_{g,\text{inf}}] > \mathbb{E}[\tau_{g,\text{symp}}]$ . Therefore, the difference between the mean serial interval and the mean infection-based generation interval is difficult to predict in general; in most cases, however, we expect the former effect to dominate, causing the mean serial interval to be longer than the mean infection-based generation interval:  $\mathbb{E}[\tau_s] > \mathbb{E}[\tau_{g,\text{inf}}]$  [2]. For simplicity, we will use the term “forward generation-interval” to refer to the infection-based generation-interval distribution (measured from a cohort of infectors who were infected at the same infection time, Fig. 1B), and drop the subscript inf.

We model the forward incubation-period  $f_I(\tau)$  and generation-interval  $f_G(\tau)$  distributions using a bivariate lognormal distribution. The joint distribution is parameterized by log means,  $\mu_I$  and  $\mu_G$ , log variances,  $\sigma_I^2$  and  $\sigma_G^2$ , and the correlation coefficient on a log scale  $\rho$ . Thus, the forward generation-interval distribution conditional on the incubation period  $f_{G|I}(\tau|\tau_{i,1})$  has a log mean of  $\mu_G + \sigma_G\rho(\log(\tau_{i,1}) - \mu_I)/\sigma_I$  and a log variance of  $\sigma_G^2(1 - \rho^2)$ . Assuming that the incidence of infection is changing exponentially at rate  $r$ , the forward serial-interval distribution  $f_S(\tau)$  for a cohort of infectors who developed symptoms at time  $t = 0$  can be calculated by integrating across infection time of the infector  $\alpha_1 < 0$  and of the infectee  $\alpha_2 > \alpha_1$  [2]:

$$f_S(\tau) = \frac{1}{\phi} \int_{-\infty}^0 \int_{\alpha_1}^\tau \exp(r\alpha_1) f_{G|I}(\alpha_2 - \alpha_1 | -\alpha_1) f_I(-\alpha_1) f_I(\tau - \alpha_2) d\alpha_2 d\alpha_1, \quad (6)$$

where  $\phi$  is a normalization constant chosen so that  $\int f_S(x) dx = 1$ ;  $-\alpha_1$  corresponds to the incubation period of the infector;  $\alpha_2 - \alpha_1$  corresponds to the generation interval; and  $\tau - \alpha_2$  corresponds to the incubation period of the infectee. As discussed earlier in Section 2.3, this method assumes that the incidence is changing exponentially at a constant rate  $r$  across the study period. As we show later in the results section, the exponential growth rate changes over the study period, including weeks 50 and 51; for illustrative purpose, we choose values of  $r$  that represent the dynamics of Delta and Omicron infections during this period and repeat the analysis across plausible ranges of  $r$  (discussed later in detail).

While the derivation of the forward serial-interval distribution Eq. (6) may be complex, its implementation is simple. The main difference between our model and

previous models that neglect dynamical effects [7, 8, 9, 10] is the exponential growth term  $\exp(r\alpha_1)$  and the normalization term  $\phi$ —it is relatively straightforward to include these terms in existing models of serial intervals. [11, 12] also included this term in their analyses of serial-interval data, but only accounted for the epidemic growth effect (and not the decay effect).

For a given value of  $r$ , we first estimate the forward incubation-period distribution from the backward distribution, previously estimated by [3], using Eq. (2). We then approximate the forward incubation-period distribution with a lognormal distribution by matching the mean and standard deviation. Using this incubation-period distribution, we fit Eq. (6) to the observed serial-interval data by minimizing the negative log-likelihood. We then calculate the mean forward generation interval using Eq. (5). The 95% confidence intervals are calculated by taking the estimated variance-covariance matrix for the log-mean and -standard deviation parameters of the log normal distributions and calculating the corresponding variance-covariance for the overall mean using Taylor expansion—this method is also known as the Delta method [13]. We assume  $\rho = 0.75$  throughout based on [14]—since we do not have individual-level data on infection and symptom onset times, we expect this parameter to be unidentifiable in practice. In Supplementary Material, we explore how assumptions about  $\rho$  affect inferences of the generation-interval distribution.

## 2.5 Estimating instantaneous reproduction number

We use our estimates of the generation-interval distributions to infer instantaneous reproduction numbers  $\mathcal{R}(t)$  of the Delta and Omicron variant, as well as the ratio between two reproduction numbers. Estimating the instantaneous reproduction number—defined as the average number of secondary infections that a primary case will generate if epidemiological conditions remain constant [15]—requires the intrinsic generation-interval distribution  $g(\tau)$ :

$$\mathcal{R}(t) = \frac{i(t)}{\int_0^\infty i(t-x)g(x) dx}, \quad (7)$$

where  $i(t)$  represents incidence of infection. Here, we approximate the intrinsic generation-interval distribution with the forward generation-interval that we estimate for weeks 50 and 51 of 2021—when the epidemic is growing or decaying exponentially, we expect the forward generation-interval to be a good proxy for the intrinsic generation-interval distribution [16, 17]. Incidence of infection is approximated by shifting the smoothed case trajectories by one week to account for reporting delays. This method of approximating incidence of infection assumes a fixed delay between infection and case reporting; in practice, deconvolution is required to accurately estimate the incidence of infection [18]. Case reports are also sensitive to changes in testing behavior, and therefore our estimates of  $\mathcal{R}(t)$  must be interpreted with care. Confidence intervals are calculated by sampling parameters of the smoothed case



trajectories as well as the generation-interval distributions from multivariate normal distributions and repeating the analysis 1000 times.

### 3 Results

Fig. 2 summarizes the epidemiological context in the Netherlands during the study period. The first known Omicron case in the Netherlands was sampled on 19 November 2021 [3], during a period when COVID-19 incidence was decreasing (Fig. 2A). As the Omicron variant continued to spread and increase in proportion (Fig. 2B), the number of COVID-19 cases started to increase (Fig. 2A). Multiplying the proportion of each variant with the number of reported COVID-19 cases further allows us to estimate the epidemiological dynamics of each (Fig. 2C). The number of COVID-19 cases caused by the Delta variant continued to decrease throughout the study period with time-varying growth rates decreasing from  $r \approx -0.01/\text{day}$  to  $r \approx -0.09/\text{day}$  by the week of January 16, 2022, and increasing back up to  $r \approx -0.04/\text{day}$  by the end of January, 2022. The number of COVID-19 cases caused by the Omicron variant increased rapidly but decelerated over time with time-varying growth rates decreasing from  $r = 0.18/\text{day}$  on the week of December 19, 2021, to  $r = 0.04/\text{day}$  by the end of January, 2022. We note that the growth-rate difference between the Delta and Omicron variants decreased over time. Hereafter, we choose  $r = -0.05/\text{day}$  for the Delta variant and  $r = 0.15/\text{day}$  for the Omicron variant as our nominal growth rates—these growth rates correspond to the mean growth rates between 1 December 2021 and 2 January 2022, during which the incubation-period data were collected. We then evaluate the growth-rate effects across  $r = -0.1/\text{day}$ – $0.0/\text{day}$  for the Delta variant and  $r = 0.1/\text{day}$ – $0.2/\text{day}$  for the Omicron variant as a sensitivity analysis.

Previous analysis of a cohort of individuals who developed symptoms between 1 December 2021 and 2 January 2022 found longer mean (backward) incubation period for the Delta variant than for the Omicron variant [3] (Fig. 3A). However, these measurements were done during a period when the incidence of Omicron was increasing while the increasing of Delta was decreasing (Fig. 2). Thus, dynamical bias would be expected to lead to shorter observed (backward) incubation periods in Omicron, and longer observed incubation periods in Delta. When we account for these growth-rate differences and re-estimate the forward incubation periods, we find that both variants have similar incubation-period distributions (Fig. 3B)—for illustrative purposes, we assume  $r = -0.05/\text{day}$  and  $r = 0.15/\text{day}$  for the Delta and Omicron variants, respectively. Although the exact estimate of the mean forward incubation periods of both variants are sensitive to the assumed growth/decay rates, we find similar means across a plausible ranges of growth rates with unclear differences between two variants (Fig. 3C–D). For example, the mean forward incubation period of the Delta variant changes from 3.8 days (95% CI: 3.5–4.1 days) to 4.4 days (95% CI: 4.0–4.8 days) as we change the assumed values of  $r$  from  $-0.1/\text{days}$  to  $0/\text{days}$  (Fig. 3C), while the mean forward incubation period of the Omicron variant

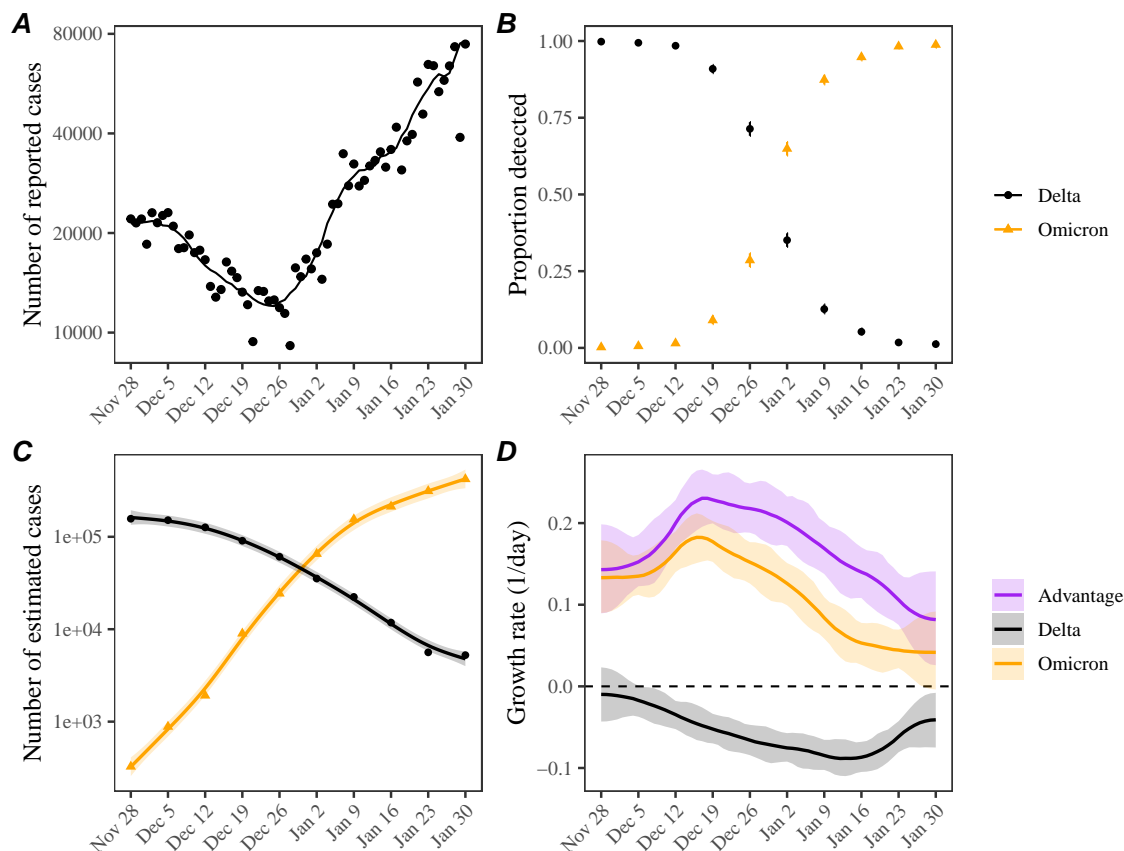


Figure 2: **Epidemic dynamics on the Delta and Omicron variants in the Netherlands between November 2021 and January 2022.** (A) Daily numbers of reported COVID-19 cases in the Netherlands (points). The solid line represents the 7-day moving average. Data are publicly available on <https://data.rivm.nl/covid-19/>. (B) Proportion of SARS-CoV-2 variants detected from the Netherlands. Data are publicly available on <https://www.rivm.nl/coronavirus-covid-19/virus/varianten>. (C) Weekly numbers of COVID-19 cases caused by the Delta (black points) and Omicron (orange triangles) variants are estimated by multiplying the weekly numbers of cases (A) with the proportion of each variant (B). Solid lines and shaded areas represent fitted lines and corresponding 95% confidence intervals using generalized additive model. (D) Estimated growth rates of the Delta (black) and Omicron variants (orange) and their growth-rate differences (purple). Lines and shaded areas represent medians and corresponding 95% confidence intervals. Growth rates are estimated by taking the derivative of the generalized additive model estimates.

changes from 3.8 days (95% CI: 3.4–4.4 days) to 4.5 days (95% CI: 3.9–5.5 days) as we change the assumed values of  $r$  from 0.1/days to 0.2/days (Fig. 3D).

Our corrected estimates of the forward incubation-period distributions further

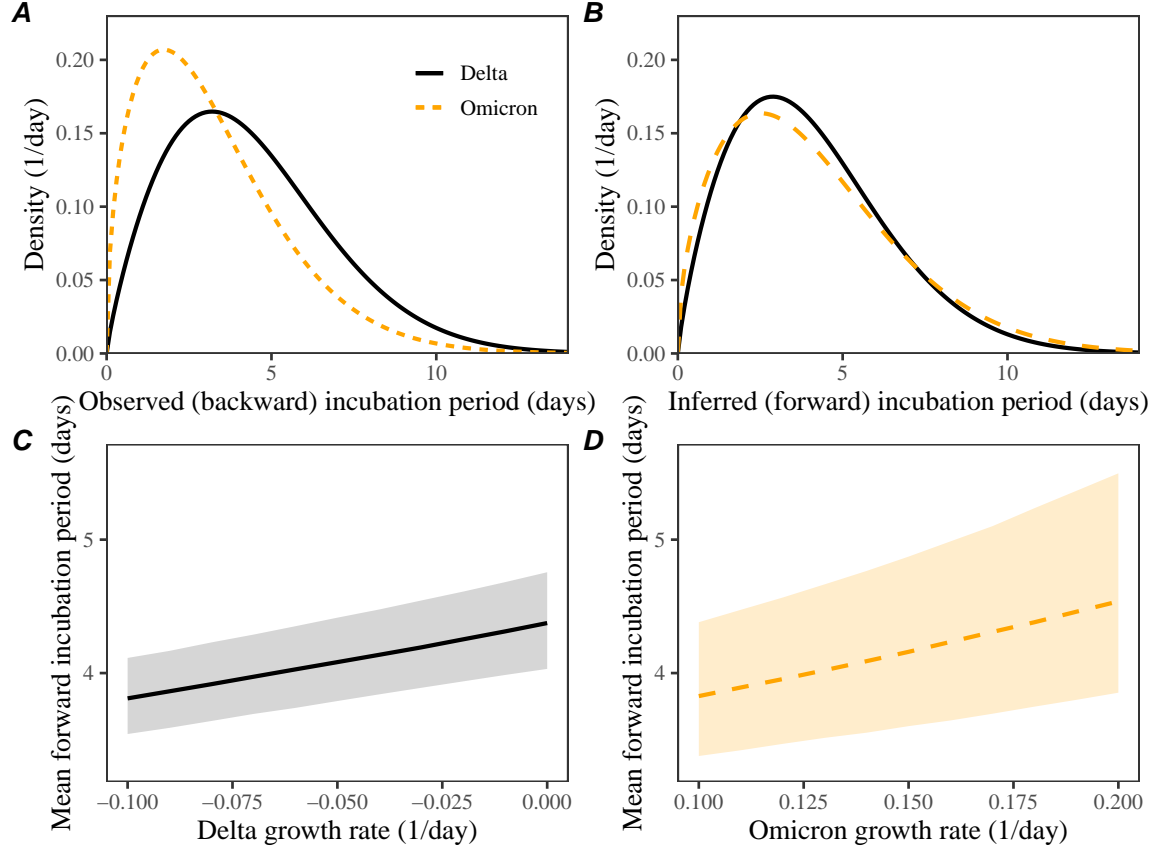


Figure 3: **Observed and corrected differences in incubation-period distributions of Delta and Omicron variants.** (A) Posterior median estimates of the observed (backward) incubation periods of the Delta (black) and Omicron (orange) variants by [3]. (B) Forward incubation-period distributions assuming  $r = -0.05/\text{day}$  and  $r = 0.15/\text{day}$  for the Delta (black) and Omicron (orange) variants, respectively. (C–D) Corrected estimates of the mean forward incubation-period for different assumptions about the growth rates of the Delta (C) and Omicron variants (D). Lines represent median estimates. Shaded regions represent the corresponding 95% confidence intervals.

allow us to infer the forward generation-interval distributions. For illustrative purposes, we first focus on aggregated serial intervals from infectors who developed symptoms during week 50–51 (13–19 December, 2021). For within-household transmission pairs (Fig. 4A), the Omicron variant has shorter mean serial interval (3.1 days; 95% CI: 2.9–3.3 days) than that of the Delta variant (3.7 days; 95% CI: 3.5–3.8 days). When we account for growth-rate differences (assuming  $r = -0.05/\text{day}$  and  $r = 0.15/\text{day}$  for the Delta and Omicron variants, respectively), the estimated mean forward generation interval exhibits a slightly larger difference (Fig. 4B): 3.0 days (95% CI: 2.7–3.2 days) for the Omicron variant and 3.8 days (95% CI: 3.7–4.0 days) for the Delta variant. Across plausible ranges of assumptions about the growth rates

of the Delta and Omicron variants, we estimate robust differences in their mean generation intervals (Fig. 4C–D). Assuming lower values of the correlation between the incubation period and generation intervals leads to larger differences in the mean generation intervals of the Delta and Omicron variants (Supplementary Figure S1).

Similar pictures arise for between-household transmission pairs, but the differences in mean serial intervals are unclear (Fig. 4E): 3.0 days (95% CI: 2.7–3.3 days) for the Omicron variant and 3.3 days (95% CI: 3.0 days–3.6 days) for the Delta variant. Consistent with the original study, which also reported shorter mean serial intervals for between-household pairs [3], we estimate shorter mean generation intervals for between-household Delta pairs. While the difference in mean generation intervals is larger, there is greater uncertainty in their mean estimates (Fig. 4F): 2.9 days (95% CI: 2.5–3.3 days) for the Omicron variant and 3.5 days (95% CI: 3.2–3.8 days) for the Delta variant. Once again, these patterns are robust across plausible ranges of assumptions about the growth rates of the Delta and Omicron variants (Fig. 4G–H).

In Supplementary Figure S2, we present generation-interval estimates that are further stratified by the week of infectors’ symptom onset (weeks 50 and 51). While we generally estimate shorter mean generation intervals for the Omicron variant, but the differences are unclear across all stratification, except for within-household transmission pairs during week 50. We also estimate a reduction in the mean forward generation intervals from week 50 to week 51 (especially for the Delta variant).

Accounting for differences in the generation-interval distributions, we estimate that the reproduction number of the Omicron variant decreased from 1.73 (95% CI: 1.59–1.89) to 1.14 (95% CI: 1.00–1.32) between December 12, 2021, and January 23, 2022 (Fig. 5A). On the other hand, the reproduction number of the Delta variant decreased from 0.90 (95% CI: 0.83–0.97) to 0.69 (95% CI: 0.65–0.75) between December 5, 2021, and January 9, 2022, and increased back up to 0.83 (95% CI: 0.73–0.94) by January 23, 2022 (Fig. 5A). We estimate the reproduction advantage (i.e., the ratio between the reproduction numbers of the Omicron and Delta variants) stayed roughly constant at around 2.10 (95% CI: 1.90–2.33) between December 12–26, 2021, and slowly decreased to 1.38 (95% CI: 1.15–1.65). However, if we neglect differences in the generation-interval distributions and solely rely on the generation-interval-distribution estimate for the Delta variant, we over-estimate the reproduction number of the Omicron variant and therefore the reproduction advantage (Fig. 5B). In this case, the reproduction advantage decreases from 2.38 (95% CI: 2.13–2.67) to 1.43 (95% CI: 1.17–1.75), corresponding to roughly 4–13% bias. Using between-household generation intervals also gives similar conclusions about changes and biases in the reproduction number estimates (Supplementary Figure S3).

In both cases, the decrease in the reproduction advantage coincides with the decrease in the reproduction number of the Omicron variant, implying that epidemiological changes driving the dynamic had larger effects on the transmission of the Omicron variant than on the transmission of Delta variant; a larger reduction in the reproduction number of the Omicron variant also caused its growth rate to decrease

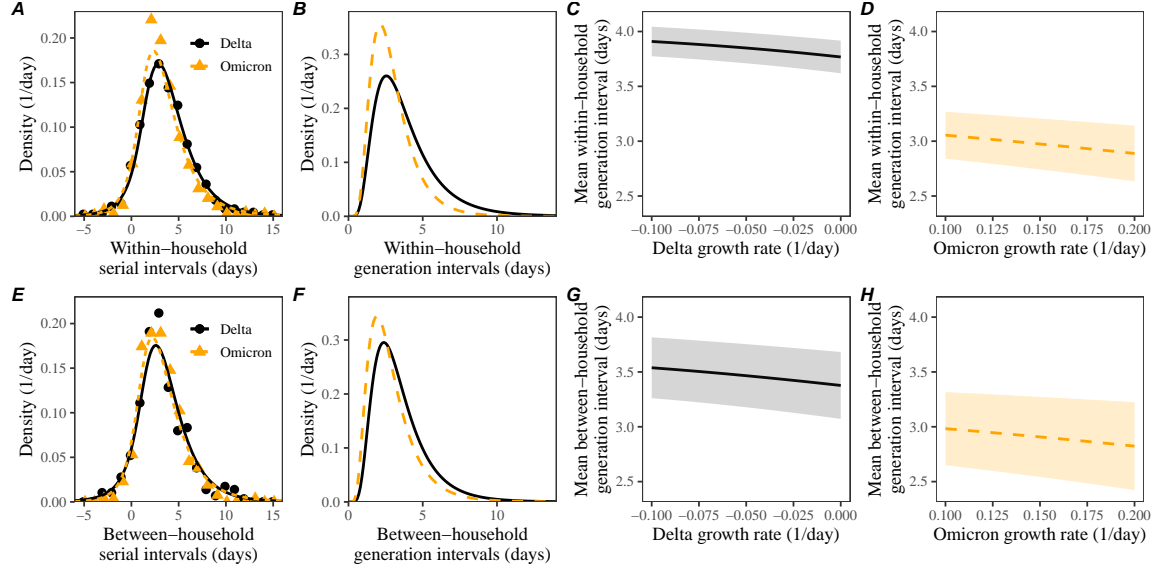


Figure 4: **Estimated forward generation-interval distributions of Delta and Omicron variants.** (A, E) Observed and fitted forward serial-interval distributions for within-household (A) and between-household (E) transmission pairs in the Netherlands for the Delta (black) and Omicron (orange) variants [3]. Serial intervals are calculated for infectors who developed symptoms on weeks 50 and 51 (13–26 December, 2021). Points represent the observed data. Lines represent the fitted lines assuming  $r = -0.05/\text{day}$  for the Delta variant and  $r = 0.15/\text{day}$  for the Omicron variant. (B, F) Estimated forward generation-interval distributions for within-household (B) and between-household (F) transmission pairs in the Netherlands. (C, D, G, H) Sensitivity of the mean forward generation-interval estimates to assumed growth rates of the Delta (C, G) and Omicron variants (G, H) for within-household (C, D) and between-household (G, H) transmission pairs. Lines represent maximum likelihood estimates. Shaded regions represent the corresponding 95% confidence intervals.

330 faster, causing changes in the observed growth-rate difference (Fig. 2D).

## 331 4 Discussion

332 We compare estimates of the forward incubation-period and generation-interval dis-  
 333 tributions of the Delta and Omicron variants from the Netherlands in late 2020 and  
 334 early 2021. The original analysis detailing the data set previously reported a shorter  
 335 mean incubation period and serial interval for the Omicron variant [3]. Accounting  
 336 for differences in epidemic growth rates, we find similar incubation-period distribu-  
 337 tions for both variants but a shorter (0.3–0.8 days) mean generation interval for the  
 338 Omicron variant relative to that of the Delta variant. Finally, we estimate that the  
 339 transmission advantage of the Omicron variant decreased from 2.1-fold to 1.4-fold

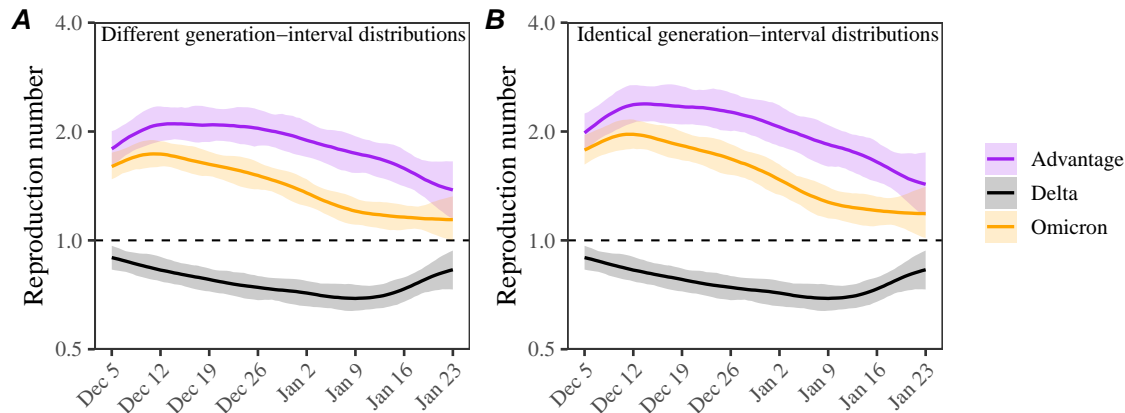


Figure 5: **Estimated time-varying reproduction number advantages of the Omicron variant.** (A) Estimated instantaneous reproduction numbers and their ratios over time while accounting for differences in the generation-interval distributions. (B) Estimated instantaneous reproduction numbers and their ratios over time while assuming identical generation-interval distributions. The instantaneous reproduction number of each variant is estimated using the renewal equation by shifting the smoothed case curves by one week (Fig. 2C). The intrinsic generation-interval distribution is approximated by the maximum likelihood estimates of the forward generation-interval distributions for within-household transmission pairs based on  $r = -0.05$  for the Delta variant (black) and  $r = 0.15$  for the Omicron variant (orange). Purple lines represent the ratio between the effective reproduction numbers of the Delta and Omicron variants. Lines and shaded regions represent medians and corresponding 95% confidence intervals.

340 between early December and late January. Our updated generation-interval esti-  
341 mates can provide more accurate understanding of epidemic dynamics and control  
342 measures.

343 The generation-interval distribution describes changes in the individual-level trans-  
344 mission dynamics over the course of infection and therefore provides crucial infor-  
345 mation for epidemic control. A few studies have estimated the generation-interval  
346 distributions of SARS-CoV-2 infections from serial-interval data, but most of them  
347 neglect the effects of epidemic growth rates [7, 8, 9, 10]—these practices can be  
348 largely attributed to historical work that concluded that serial and generation inter-  
349 vals have the same means based on the assumption that infectors and infectees have  
350 identical incubation-period distributions [19, 20, 21]. Here, we build on previous  
351 work [2], which demonstrated theoretically that forward serial-interval distributions  
352 depends on epidemic growth rates, and further confirm that estimates of the forward  
353 generation-interval distributions are indeed sensitive to epidemic growth rates. Ac-  
354 counting for the growth-rate effects is especially important when comparing serial  
355 and generation intervals of different variants or from different time periods. These  
356 effects are also pertinent to epidemiological inferences of past events from a cohort

357 of infected individuals who experienced the succeeding event at the same time—this  
 358 includes inferences of other delay distributions, such as incubation-period distribu-  
 359 tions, as well as viral load trajectories [22]. Our sensitivity analysis also shows that  
 360 the assumptions about the correlation between incubation periods and generation  
 361 intervals can also have important effects on the estimates of the generation-interval  
 362 distributions (Supplementary Figure S1).

363 A few studies have suggested the the incubation period of the Omicron variant  
 364 may be shorter than that of the Delta variant. The median estimates of the Omicron  
 365 incubation period typically range between 3–4 days, consistent with earlier findings  
 366 of [3]. However, these data were collected when the number of Omicron infections  
 367 was growing rapidly [23, 24], suggesting that they may have been subject to similar  
 368 biases. On the other hand, incubation-period estimates based on individuals who  
 369 were exposed from the same event are likely more reliable (because they look forward  
 370 in time): [25] estimated the median incubation period of the Omicron variant to be  
 371 3 days among those who attended the same holiday party ( $n = 117$ ) on 26 November  
 372 2021 in Norway. However, we cannot rule out the possibility that some of these  
 373 attendees were infected prior to the party given that some individuals had COVID-  
 374 like symptoms prior to the party with at least 96 of the attendees sharing offices;  
 375 neglecting these factors can lead to underestimation of the mean incubation period.  
 376 Systematic comparisons of data collection methods and epidemiological contexts are  
 377 needed to properly assess the differences in incubation period distributions of the  
 378 Delta and Omicron variants.

379 A few studies have estimated that the Omicron variant has shorter transmis-  
 380 sion intervals than the Delta variant [1, 26, 24], but there has been a lack of direct  
 381 generation-interval estimates. [27, 28] tried to estimate the generation-interval dis-  
 382 tributions of the Omicron variant but they both relied on population-level epidemic  
 383 dynamics (rather than individual-level transmission data). To our knowledge, our  
 384 study is the first to estimate the generation-interval distribution of the Omicron  
 385 variant from serial-interval data. Although we estimate a shorter mean generation  
 386 interval for the Omicron variant, we find the generation-interval distribution of the  
 387 Omicron and Delta variants have similar modes (around 2.5 days), implying that the  
 388 realized transmissibility of the Omicron variant decays faster. We tentatively hypoth-  
 389 esize that these differences may be primarily driven by the network effect [17, 10]: a  
 390 higher reproduction numbers of the Omicron variant leads to faster susceptible de-  
 391 pletion among close contacts, which in turn prevents long generation intervals from  
 392 generating infections. While the network effect is expected to be strongest among  
 393 household contacts, it is also applicable to other forms of contact structures that  
 394 involve repeated contacts between the same group of individuals (because only the  
 395 first infectious contact results in infection). The network effect may also explain a  
 396 decrease in the mean generation interval between week 50 and 51, especially among  
 397 household transmission pairs, as a higher proportion of individuals within house-  
 398 holds would have been infected with either the Delta or Omicron variants. Shorter  
 399 generation-interval estimates for between-household contacts may be attributable to

behavioral effects: individuals who have symptoms or tested positive may be more likely to stay home, preventing long between-household transmission. Other factors, such as more stringent intervention measures against the Omicron variant [3] and faster within-host clearance of the Omicron variant [29], also likely contributed to shortening of generation intervals.

While our study indicates that the Omicron variant has a shorter mean realized generation interval than that of the Delta variant, it is still uncertain how infectiousness profiles differ intrinsically between Omicron and Delta. In particular, similarities in the incubation-period distributions of the Delta and Omicron variants suggest that the differences in their true infectiousness profile may be smaller than the estimated differences in their realized generation-interval distributions. In addition, the unmitigated generation intervals of both Omicron and Delta variants are likely longer than what we estimate given existing levels of interventions, including vaccination, and pandemic awareness—estimating “unmitigated” or “intrinsic” generation-interval distributions of SARS-CoV-2 variants are expected to be a difficult problem as it requires early data during which interventions and awareness levels were minimal [14]. Nonetheless, our estimates of the realized generation-interval distributions better describe current epidemic dynamics, implicitly accounting for intervention and behavioral effects. Therefore, our generation-interval estimates are expected to give more accurate estimates of reproduction numbers.

Our study also has important implications for estimating transmission advantages of new SARS-CoV-2 variants. In the example we consider, neglecting differences in the generation-interval distributions leads to  $\approx 10\%$  bias in the estimates of the reproduction advantage (i.e., the ratio between the reproduction numbers of the Omicron and Delta variants). More generally, the bias in inferring the reproduction advantage an emerging variant is expected to be sensitive to the assumed generation-interval distribution of the resident variant. For example, [30] estimated a much higher reproduction advantage of the Omicron variant ( $> 4$  fold) compared to the Delta variant in South Africa but also assumed a longer mean generation interval for the Delta and Omicron variants (6.4 vs 5.2 days, respectively). With our generation-interval estimates, we estimate that the reproduction advantage of 2.6 for the Omicron variant assuming  $r = -0.06$  and  $r = 0.26$  for the Delta and Omicron variants, respectively—these growth rates were chosen to match the 4-fold reproduction advantage with the estimated growth-rate differences of 0.32/day for the Gauteng province, South Africa [30].

We considered two ways of measuring transmission advantages: growth-rate differences and reproduction advantage. Characterizing new variants in terms of their reproduction advantage is useful because it is directly related to the amount of increased transmissibility and immune evasion [30]. On the other hand, the growth-rate difference likely provides a better measure for transmission advantage for an ongoing epidemic as it provides information about which strain is growing faster. For example, when two strains have the same  $\mathcal{R}$ , the one with shorter generation intervals will grow faster and replace the other strain—this transmission advantage is cap-



443 tured by the growth-rate difference, but not by the ratio of reproduction numbers  
444 of two strains. Therefore, we suggest using growth-rate differences and reproduction  
445 advantage as complementary measures for understanding the dynamics of emerging  
446 SARS-CoV-2 variants.

447 We primarily rely on case data to understand epidemic patterns of the Delta and  
448 Omicron variants. In doing so, we implicitly assume that the delay between infection  
449 and reports is fixed. However, changes in case trajectories are sensitive to testing  
450 patterns and therefore may not accurately reflect patterns of infections. While this  
451 limitation does not affect our generation-interval estimates, our inferences of the  
452 transmission advantages of the Omicron variant should be interpreted with care.

453 Monitoring changes in key epidemiological parameters is critical to understand-  
454 ing the evolution of SARS-CoV-2 and predicting its future dynamics [31]. Our study  
455 synthesizes a previously developed theoretical framework on serial- and generation-  
456 interval distributions and presents methodological advances in monitoring epidemi-  
457 ological parameters. Similar efforts will be critical to improve estimates of the infec-  
458 tiousness profiles of future SARS-CoV-2 variants, especially among asymptotically  
459 infected individuals [32].

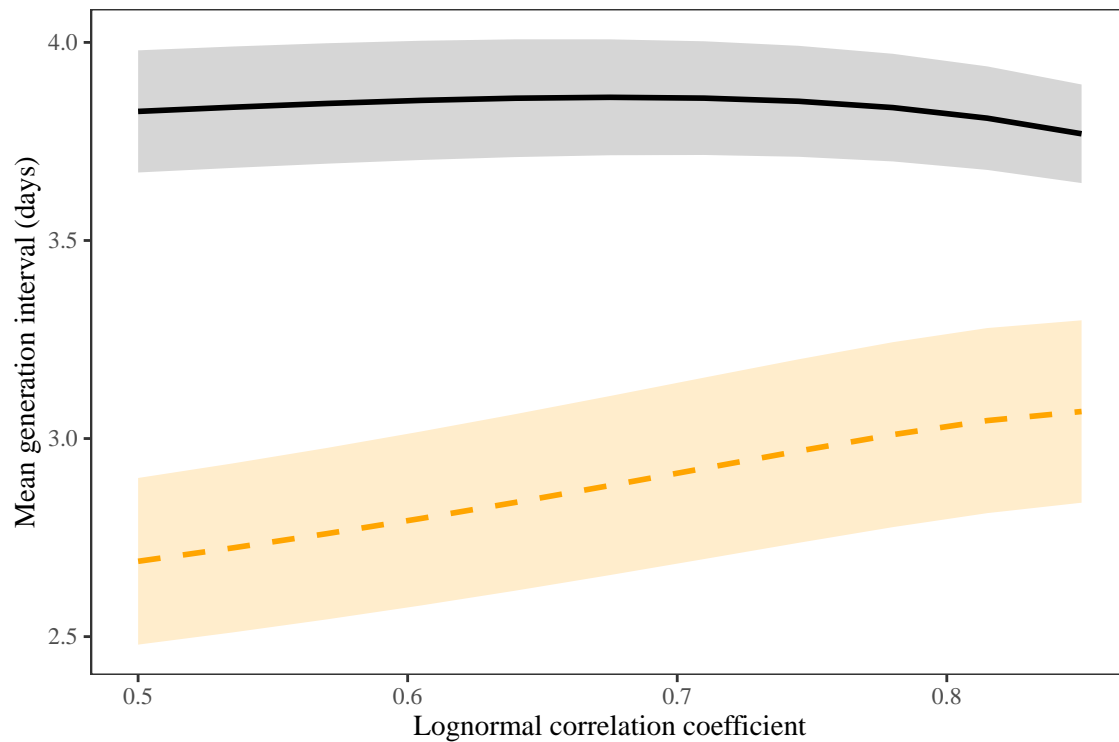


Figure S1: **Sensitivity of the estimates of the mean generation interval to the assumed values of the correlation coefficient of the lognormal distribution.** Lines and shaded regions represent maximum likelihood estimates and the corresponding 95% confidence intervals for the Delta (black, solid lines) and Omicron variants (orange, dashed lines). For illustrative purposes we use within-household serial-interval data from the cohort of infectors who developed symptoms during weeks 50 and 51 of 2021.

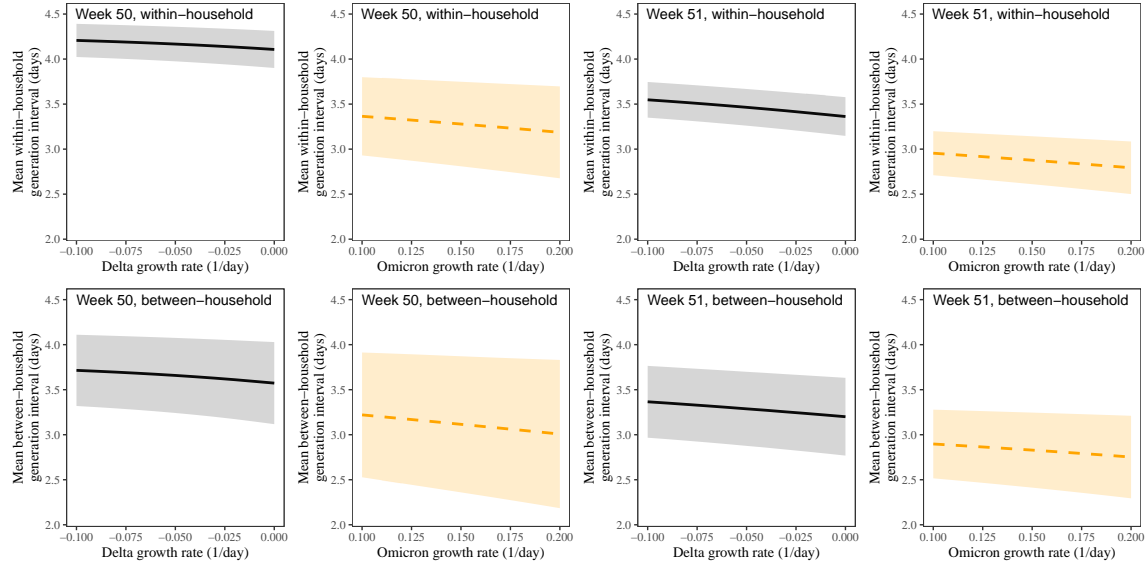


Figure S2: **Estimated mean forward generation intervals of Delta and Omicron variants across different stratifications.** Sensitivity of the mean forward generation-interval estimates to assumed growth rates of the Delta and Omicron variants stratified by the types of transmission (within- vs between-household transmission) and the week of infectors' symptom onset (weeks 50 vs 51 of 2021). Lines represent maximum likelihood estimates. Shaded regions represent the corresponding 95% confidence intervals.

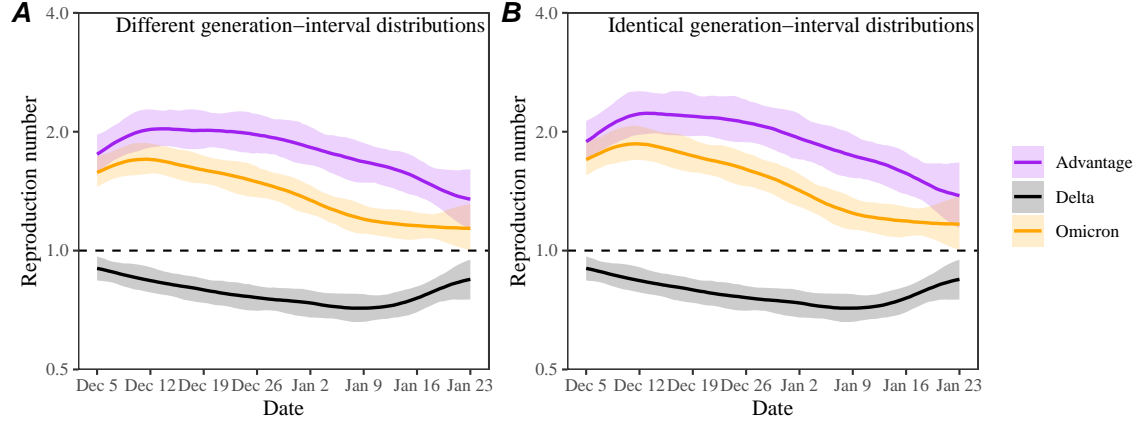


Figure S3: **Estimated time-varying reproduction number advantages of the Omicron variant using between-household generation-interval distributions.** (A) Estimated instantaneous reproduction numbers and their ratios over time while accounting for differences in the generation-interval distributions. (B) Estimated instantaneous reproduction numbers and their ratios over time while assuming identical generation-interval distributions. The instantaneous reproduction number of each variant is estimated using the renewal equation by shifting the smoothed case curves by one week (Fig. 2C). The intrinsic generation-interval distribution is approximated by the maximum likelihood estimates of the forward generation-interval distributions for between-household transmission pairs based on  $r = -0.05$  for the Delta variant (black) and  $r = 0.15$  for the Omicron variant (orange). Purple lines represent the ratio between the effective reproduction numbers of the Delta and Omicron variants. Lines and shaded regions represent medians and corresponding 95% confidence intervals.

## References

- [1] Sam Abbott, Katharine Sherratt, Moritz Gerstung, and Sebastian Funk. Estimation of the test to test distribution as a proxy for generation interval distribution for the Omicron variant in England. *medRxiv*, 2022.
- [2] Sang Woo Park, Kaiyuan Sun, David Champredon, Michael Li, Benjamin M Bolker, David JD Earn, Joshua S Weitz, Bryan T Grenfell, and Jonathan Dushoff. Forward-looking serial intervals correctly link epidemic growth to reproduction numbers. *Proceedings of the National Academy of Sciences*, 118(2), 2021.
- [3] Jantien A Backer, Dirk Eggink, Stijn P Andeweg, Irene K Veldhuijzen, Noortje van Maarseveen, Klaas Vermaas, Boris Vlaemynck, Raf Schepers, Susan van den Hof, Chantal BEM Reusken, and Jacco Wallinga. Shorter serial intervals in SARS-CoV-2 cases with Omicron BA.1 variant compared with Delta variant, the Netherlands, 13 to 26 December 2021. *Eurosurveillance*, 27(6):2200042, 2022.
- [4] Simon N Wood. mgcv: GAMs and generalized ridge regression for R. *R News*, 1(2):20–25, 2001.
- [5] Jantien A Backer, Don Klinkenberg, and Jacco Wallinga. Incubation period of 2019 novel coronavirus (2019-nCoV) infections among travellers from Wuhan, China, 20–28 January 2020. *Eurosurveillance*, 25(5):2000062, 2020.
- [6] Sang Woo Park, Benjamin M Bolker, David Champredon, David JD Earn, Michael Li, Joshua S Weitz, Bryan T Grenfell, and Jonathan Dushoff. Reconciling early-outbreak estimates of the basic reproductive number and its uncertainty: framework and applications to the novel coronavirus (SARS-CoV-2) outbreak. *Journal of the Royal Society Interface*, 17(168):20200144, 2020.
- [7] Tapiwa Ganyani, Cecile Kremer, Dongxuan Chen, Andrea Torneri, Christel Faes, Jacco Wallinga, and Niel Hens. Estimating the generation interval for coronavirus disease (COVID-19) based on symptom onset data, March 2020. *Eurosurveillance*, 25(17):2000257, 2020.
- [8] Xi He, Eric HY Lau, Peng Wu, Xilong Deng, Jian Wang, Xinxin Hao, Yiu Chung Lau, Jessica Y Wong, Yujuan Guan, Xinghua Tan, et al. Temporal dynamics in viral shedding and transmissibility of COVID-19. *Nature medicine*, 26(5):672–675, 2020.
- [9] Shi Zhao, Biao Tang, Salihu S Musa, Shujuan Ma, Jiayue Zhang, Minyan Zeng, Qingping Yun, Wei Guo, Yixiang Zheng, Zuyao Yang, et al. Estimating the generation interval and inferring the latent period of COVID-19 from the contact tracing data. *Epidemics*, 36:100482, 2021.

- [10] William S Hart, Elizabeth Miller, Nick J Andrews, Pauline Waight, Philip K Maini, Sebastian Funk, and Robin N Thompson. Generation time of the alpha and delta SARS-CoV-2 variants: an epidemiological analysis. *The Lancet Infectious Diseases*, 2022.
- [11] Luca Ferretti, Chris Wymant, Michelle Kendall, Lele Zhao, Anel Nurtay, Lucie Abeler-Dörner, Michael Parker, David Bonsall, and Christophe Fraser. Quantifying SARS-CoV-2 transmission suggests epidemic control with digital contact tracing. *Science*, 368(6491):eabb6936, 2020.
- [12] Luca Ferretti, Alice Ledda, Chris Wymant, Lele Zhao, Virginia Ledda, Lucie Abeler-Dörner, Michelle Kendall, Anel Nurtay, Hao-Yuan Cheng, Ta-Chou Ng, et al. The timing of COVID-19 transmission. *medRxiv*, 2020.
- [13] Gary W Oehlert. A note on the Delta method. *The American Statistician*, 46(1):27–29, 1992.
- [14] Ron Sender, Yinon M Bar-On, Sang Woo Park, Elad Noor, Jonathan Dushoffd, and Ron Milo. The unmitigated profile of COVID-19 infectiousness. *medRxiv*, 2021.
- [15] Christophe Fraser. Estimating individual and household reproduction numbers in an emerging epidemic. *PloS one*, 2(8):e758, 2007.
- [16] David Champredon and Jonathan Dushoff. Intrinsic and realized generation intervals in infectious-disease transmission. *Proceedings of the Royal Society B: Biological Sciences*, 282(1821):20152026, 2015.
- [17] Sang Woo Park, David Champredon, and Jonathan Dushoff. Inferring generation-interval distributions from contact-tracing data. *Journal of the Royal Society Interface*, 17(167):20190719, 2020.
- [18] Edward Goldstein, Jonathan Dushoff, Junling Ma, Joshua B Plotkin, David JD Earn, and Marc Lipsitch. Reconstructing influenza incidence by deconvolution of daily mortality time series. *Proceedings of the National Academy of Sciences*, 106(51):21825–21829, 2009.
- [19] Åke Svensson. A note on generation times in epidemic models. *Mathematical biosciences*, 208(1):300–311, 2007.
- [20] Tom Britton and Gianpaolo Scalia Tomba. Estimation in emerging epidemics: biases and remedies. *Journal of the Royal Society Interface*, 16(150):20180670, 2019.
- [21] Sonja Lehtinen, Peter Ashcroft, and Sebastian Bonhoeffer. On the relationship between serial interval, infectiousness profile and generation time. *Journal of the Royal Society Interface*, 18(174):20200756, 2021.

- [22] James A Hay, Lee Kennedy-Shaffer, Sanjat Kanjilal, Niall J Lennon, Stacey B Gabriel, Marc Lipsitch, and Michael J Mina. Estimating epidemiologic dynamics from cross-sectional viral load distributions. *Science*, 373(6552):eabh0635, 2021.
- [23] Lauren Jansen, Bryan Tegomoh, Kate Lange, Kimberly Showalter, Jon Figliomeni, Baha Abdalhamid, Peter C Iwen, Joseph Fauver, Bryan Buss, and Matthew Donahue. Investigation of a Sars-Cov-2 B.1.1.529 (Omicron) variant cluster—Nebraska, November–December 2021. *Morbidity and Mortality Weekly Report*, 70(5152):1782, 2021.
- [24] Jin Su Song, Jihee Lee, Miyoung Kim, Hyeong Seop Jeong, Moon Su Kim, Seong Gon Kim, Han Na Yoo, Ji Joo Lee, Hye Young Lee, Sang-Eun Lee, et al. Serial intervals and household transmission of SARS-CoV-2 Omicron variant, South Korea, 2021. *Emerging Infectious Diseases*, 28(3):756, 2022.
- [25] Lin T Brandal, Emily MacDonald, Lamprini Veneti, Tine Ravlo, Heidi Lange, Umaer Naseer, Siri Feruglio, Karoline Bragstad, Olav Hungnes, Liz E Ødeskaug, et al. Outbreak caused by the SARS-CoV-2 Omicron variant in Norway, November to December 2021. *Eurosurveillance*, 26(50):2101147, 2021.
- [26] Cécile Kremer, Toon Braeye, Kristiaan Proesmans, Emmanuel André, Andrea Torneri, and Niel Hens. Observed serial intervals of SARS-CoV-2 for the Omicron and Delta variants in Belgium based on contact tracing data, 19 November to 31 December 2021. *medRxiv*, 2022.
- [27] Kimihito Ito, Chayada Piantham, and Hiroshi Nishiura. Estimating relative generation times and relative reproduction numbers of Omicron BA.1 and BA.2 with respect to Delta in Denmark. *medRxiv*, 2022.
- [28] Alex Selby. Estimating generation time of Omicron. 2022.
- [29] James A Hay, Stephen M Kissler, Joseph R Fauver, Christina Mack, Caroline G Tai, Radhika M Samant, Sarah Connelly, Deverick J Anderson, Gaurav Khullar, Matthew MacKay, et al. Viral dynamics and duration of PCR positivity of the SARS-CoV-2 Omicron variant. *medRxiv*, 2022.
- [30] Carl AB Pearson, Sheetal P Silal, Michael WZ Li, Jonathan Dushoff, Benjamin M Bolker, Sam Abbott, Cari van Schalkwyk, Nicholas G Davies, Rosanna C Barnard, W John Edmunds, et al. Bounding the levels of transmissibility & immune evasion of the Omicron variant in South Africa. *MedRxiv*, 2021.
- [31] Moritz UG Kraemer, Oliver G Pybus, Christophe Fraser, Simon Cauchemez, Andrew Rambaut, and Benjamin J Cowling. Monitoring key epidemiological parameters of SARS-CoV-2 transmission. *Nature medicine*, 27(11):1854–1855, 2021.

- 571 [32] Sang Woo Park, Daniel M Cornforth, Jonathan Dushoff, and Joshua S Weitz.  
572 The time scale of asymptomatic transmission affects estimates of epidemic po-  
573 tential in the COVID-19 outbreak. *Epidemics*, 31:100392, 2020.